SPH Modelling of Plunging Wave Breaking, Surf Zone Turbulence and Wave-Induced Currents

Christos V. Makris *&* ***Yannis N. Krestenitis****, Aristotle University of Thessaloniki, Greece*
Constantine D. Memos*, National Technical University of Athens, Greece*

Following our previous work (Makris *et al.*, 2010), SPHysics code v.2 (Gómez-Gesteira *et al.*, 2010) has been thoroughly calibrated and validated against experimental data for wave propagation and weak plunging breaking on a smooth mild sloping beach placed inside a laboratory scale wave flume (Stansby & Feng, 2005). The LES-type Smagorinsky model is used for the viscosity treatment. Spatial resolution is based on the size of expected turbulent eddies. Discretization values Δx approach the demarcation range between integral turbulence length scales (energy-containing eddies) and Taylor micro-scales (inertial sub-range).

Remarkable visual output (Fig. 1) is further supported by extended quantitative validation through comparison between experimental data and SPHysics results. In this framework, several classic and more sophisticated hydrodynamic features are investigated. Plausible agreement is achieved in terms of wave heights and setup, r.m.s. free-surface elevation fluctuation, wave crest and trough envelopes, throughout the whole computational domain (Fig. 2). Relevant Pearson correlation coefficients vary from 0.9 to 0.97 for most cases. Moreover, ensemble-averaged free-surface elevation and depth-averaged velocities are generally well predicted (Fig. 3).

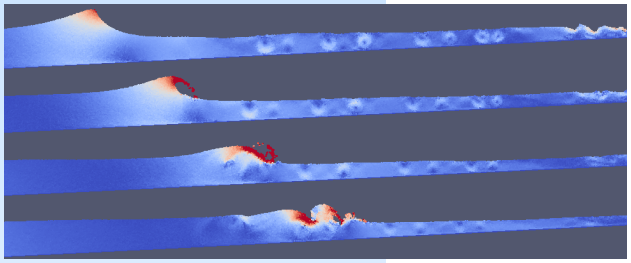

Figure 1 – Consecutive depictions (PV-Meshless) of simulated (SPHysics) weak plunging wave breaking and consequent turbulent bore formation.

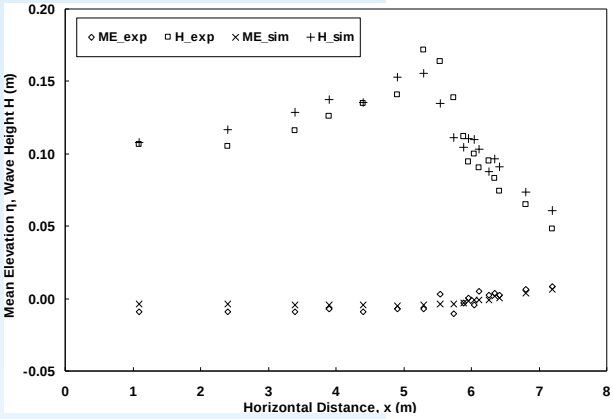

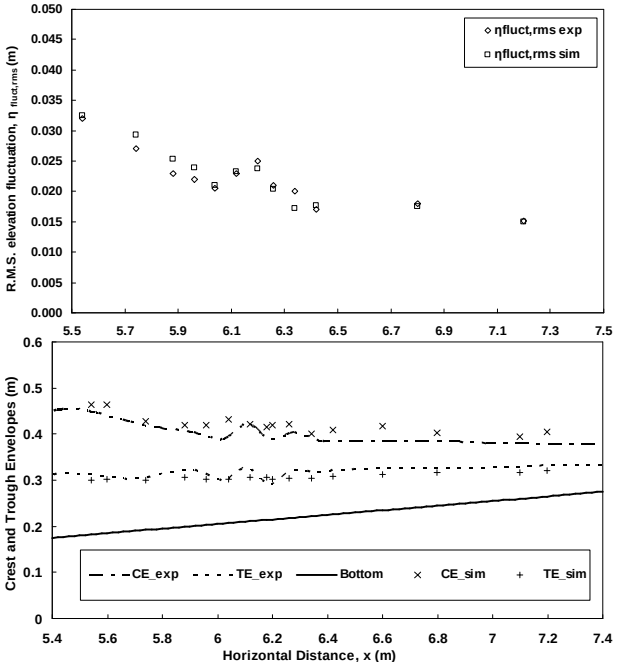

Figure 2 – Comparison between experimental data (exp) and SPHysics output (sim), for wave heights and setup [bottom of previous page], r.m.s. free-surface elevation fluctuation [upper], wave crest and trough envelopes [lower].

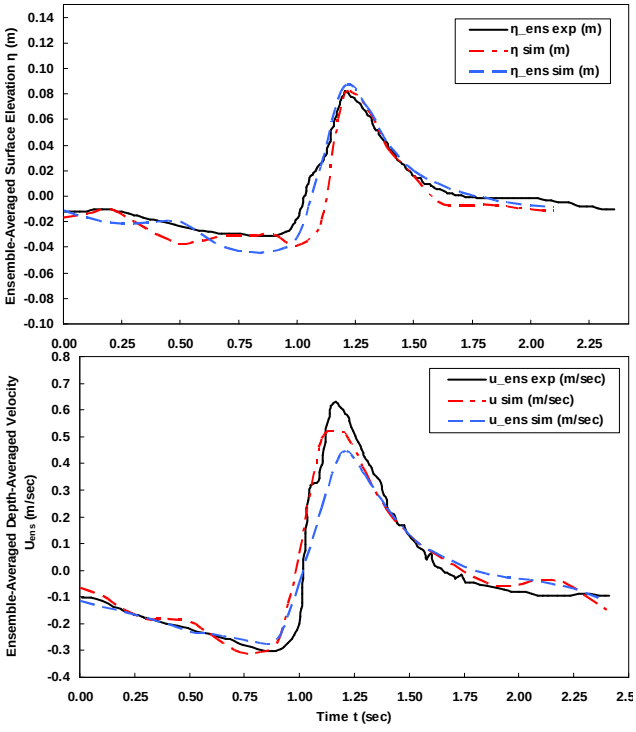

Figure 3 – Comparison of experimental (exp) against SPHysics (sim) output for ensemble-averaged (blue dash) and real-time (red dash-dot) values of free-surface elevation [upper] and depth-averaged velocity [lower].

The Fourier spectra of the simulated turbulent component of horizontal velocities **u´** at still surface level is derived (Fig. 4), revealing a trend that follows the –5/3 slope on the log/log scale, typical of isotropic (inertial sub-range) turbulence. This is the case for turbulent wavenumber values of f = 10Hz, somehow continued until the Nyquist filter limit f = 25Hz. Improvement of our previous results (Makris *et al.*, 2010) is clear for high frequency bands, that correspond to either the SPS-treated scales or the smaller of the resolved large eddies. Besides that, preliminary results of residual normal and shear stresses reveal a mild anisotropy in turbulence especially in the vicinity of the initial plunging breaking region.

In addition, we focus on the simulation of the wave-induced mean flows in the surf zone, namely the undertow and the Stokes drift (Fig. 5). The period-averaged kinematics for the surf zone is very similar to that of Stansby & Feng (2005), for velocity vector field averaging both over the 'wet' period (the time for which a point is immersed in water for a wave cycle) and the actual one. Moreover, the shoreward inversion of the mean flow near the bed (streaming), is qualitatively well predicted by SPHysics. Depth-averaged horizontal volume flux over one period is close to zero, indicating an acceptable level of accuracy for our simulations.

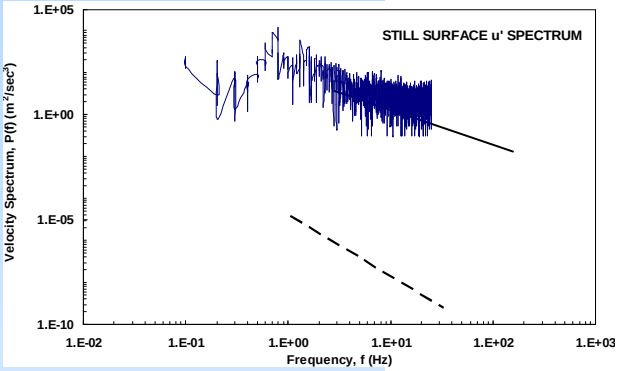

Figure 4 – Fourier spectra of simulated turbulent component of horizontal velocity **u´** for the incipient breaking region at still surface level.

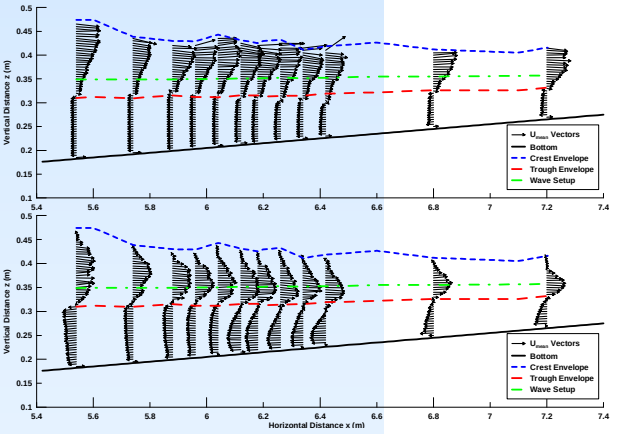

Figure 5 – Time-averaged vertical distribution of velocity at gauges in the surf zone for 'wet period' [upper] and real-time [lower] data. Depiction of undertow and Stokes' drift regions, delimited by envelopes of wave trough (red dash), crest (blue dash), and setup (green dash-dot).

Recurring patterns of periodically concentrated vorticity in a 2D cross-sectional plane are investigated too (Fig. 6). Evolution of the relevant vorticity field is similar to that of experiments (Stansby & Feng, 2005; Nadaoka *et al.*, 1989). The period-averaged values are as expected with a thick layer of clockwise (positive) vorticity around the trough level and counter-clockwise (negative) near the bed (lower Fig. 6). Concentrated ensemble-averaged vorticity is also apparent in the surf zone (roller, plunger and bore regions) shown as multiple turbulent coherent structures (Fig. 7).

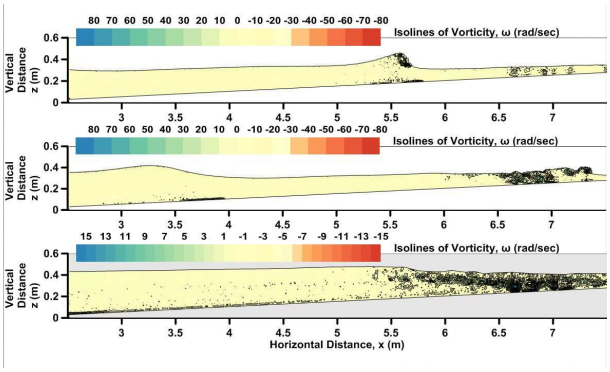

Figure 6 – Recurring vortical patterns during wave breaking [upper graphs]. Period-averaged vorticity field (coherent turbulent structures) [lower].

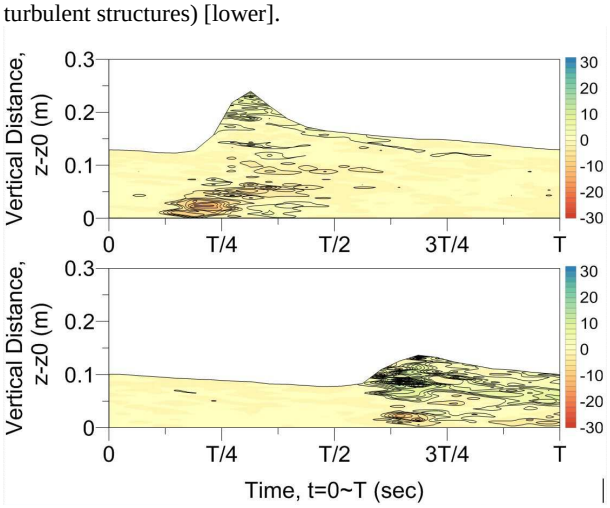

Figure 7 – Ensemble-averaged vorticity contours (coherent turbulent structures) at gauges in the incipient breaking region [upper] and inner surf zone [lower].

Contact: cmakris@civil.auth.gr

References

Gómez-Gesteira, M., Rogers, B.D., Dalrymple, R.A., Crespo, A.J.C., Narayanaswamy, M. (2010), *User guide for the SPHysics code v2.0*.

Makris, C.V., Krestenitis, Y.N., Memos, C.D. (2010), *SPHysics code validation against a near-shore wave breaking experiment*, Proc. 5th SPHERIC Int. Workshop, pp. 245–252.

Nadaoka, K., Hino, M., Koyano, Y. (1989), *Structure of the turbulent flow field under breaking waves in the surf zone*, J. Fluid Mech. **204**:359–387.

Stansby, P.K., Feng, T. (2005), *Kinematics and depth-integrated terms in surf zone waves from laboratory measurement*. J. Fluid Mech. **529**:279–310.